Zircon O- and Hf-isotope constraints on the genesis and tectonic significance of Permian magmatism in Patagonia

Paula Castillo[1*], C. Mark Fanning[1], Robert J. Pankhurst[2], Francisco Hervé[3] & Carlos W. Rapela[4]

[1] Research School of Earth Sciences, The Australian National University, Canberra, ACT 0200, Australia
[2] British Geological Survey, Keyworth NG12 5GG, UK
[3] Carrera de Geología, Universidad Andres Bello, Sazie 2119, Santiago, Chile
[4] Centro de Investigaciones Geológicas, Diagonal 113, Calle 64, 1900 La Plata, Argentina
 P.C., 0000-0003-1090-6511; R.J.P., 0000-0001-6167-5210; C.W.R., 0000-0002-3478-2229
* Correspondence: paula.castillo@anu.edu.au

Abstract: The genesis of Permian magmatism in southern South America is actively debated, particularly in relation to the origin of Patagonia. U–Pb zircon ages of *c.* 255 Ma for igneous rocks from the basement of Tierra del Fuego are the first evidence for southerly prolongation of this magmatism. Zircon in these rocks has εHf_t values <-1 and $\delta^{18}O > 7.4‰$, indicating recycling of Cambrian rocks. Permian granites in the north of the North Patagonian Massif record mantle-like $\delta^{18}O$ magmatic input at *c.* 280 and 255 Ma, but reworking of upper crust between these two events, paralleling the recognized deformational history. In northwestern Patagonia, Early Permian granitic rocks have zircon with εHf_t values ranging from $+0.1$ to -7.2, and $\delta^{18}O > 6.2‰$, suggesting continuity of the Permian magmatic belt along the western margin of South America farther north. Comparison with a sample from the Sierra de la Ventana suggests melting of similar crust on both sides of the Patagonia–South American hypothetical suture. These features, together with other geological considerations, are consistent with an autochthonous or parautochthonous origin of northern Patagonia and connection between southern Patagonia and the Antarctic Peninsula in late Palaeozoic time.

Supplementary material: U–Pb SHRIMP, O and Hf analytical data are available at https://doi.org/10.6084/m9.figshare.c.3768710

Received 5 December 2016; **revised** 23 February 2017; **accepted** 7 March 2017

The origin and tectonic evolution of the southern part of South America is still actively debated. Discussions not only focus on whether Patagonia has always been part of South America or an accreted crustal block (e.g. Ramos 1984, 2008; Pankhurst *et al.* 2006; Rapalini *et al.* 2013; Ramos & Naipauer 2014), but also include uncertainty about its uniformity (e.g. Pankhurst *et al.* 2006; Schilling *et al.* 2008; Chernicoff *et al.* 2013; Mundl *et al.* 2015) and its relationship with other crustal blocks such as the Antarctic Peninsula (e.g. Hervé *et al.* 2005; Castillo *et al.* 2016). Permian plutonic and volcanic rocks are widespread in northern Patagonia and constitute an excellent tool to examine the different hypotheses on the origin of Patagonia. One hypothesis considers the whole of Patagonia as an allochthonous terrane, originating on the East Antarctic margin that collided with Gondwana (South America) in the late Palaeozoic (Ramos 1984, 2008; Ramos & Naipauer 2014). In the current form of this model, the movement of Patagonia towards Gondwana and the subsequent collision during the late Permian gave rise to this significant magmatic event. The second hypothesis considers northern Patagonia to be autochthonous, and the central and southern parts to be allochthonous (Pankhurst *et al.* 2006). In this case, the Permian magmatism is assigned to a subducted slab break-off under northern Patagonia after the collision of southern Patagonia. Although deformation in the northeastern corner of the North Patagonian Massif, with a major NNE–SSW compressive stress regime, supports a collision as in the first model (von Gosen 2003; López de Luchi *et al.* 2010), Cambrian and Ordovician granites in the same area point towards a continuation of the Pampean and Famatinian orogenic belts of South America (Rapalini *et al.* 2013; Pankhurst *et al.* 2014). In an attempt to reconcile evidence for both autochthony and collision,

Rapalini (2005) introduced a parautochthonous model, in which Patagonia first rifted from South America, as suggested by Rapela *et al.* (2003), and later re-collided.

In this study, new and published U–Pb sensitive high-resolution ion microprobe (SHRIMP) zircon ages have been supplemented and integrated with Hf- and O-isotope data for Permian granitoids from northern and southern Patagonia. The aim is to re-evaluate Permian crustal evolution in Patagonia, place constraints on the tectonic activity, and test different tectonic models as well as possible connection with the Antarctic Peninsula. The combined analysis of the stable O and radiogenic Hf isotopic compositions in zircon provides valuable information about aspects of granite genesis, in particular the relative contributions of juvenile depleted mantle and recycled or longer-lived crustal sources in the magmatic system (e.g. Hawkesworth & Kemp 2006; Kemp *et al.* 2007). Magmas with long crustal residence after extraction from depleted mantle normally interact with other isotopic reservoirs from the crust. In this case, the time-dependent Hf isotope compositions can be coupled with O-isotope data, the latter being very sensitive to additions or mixing with crustal sources (Hawkesworth & Kemp 2006; Kemp *et al.* 2006, 2007). However, Hf and O isotopes are not always correlated. If a mantle-derived magma crystallizes and then remains in the deep crust without interacting with upper crustal material, the O isotopic compositions will retain their mantle-like compositions but the Hf isotopic compositions would continue to evolve by radioactive decay (albeit rather more slowly than in depleted mantle owing to the lower Lu/Hf ratio). If new magma is subsequently formed from this source, zircon crystallizing from it would inherit mantle-type O but more evolved Hf isotopic compositions. Thus the O and Hf isotopes would have become decoupled, Hf appearing to indicate an

older crustal component whereas O would indicate the essentially juvenile origin. Hence we stress the need to use both Hf and O systematics for such studies.

Geological setting

Patagonia is the geographical region south of Río Colorado (Fig. 1). It consists of the Patagonian and Fuegian segments of the Andes on the Pacific side and a platform known as extra-Andean Patagonia, which extends eastwards from the Andes to the Atlantic coast. The crystalline Palaeozoic basement of Patagonia has been traditionally considered in terms of two tectonic blocks: the North Patagonian Massif (NPM) and the Deseado Massif. The NPM occupies most of northern Patagonia (Fig. 1). Its northern boundary is covered by the Meso-Cenozoic Colorado Basin (Yrigoyen 1999), but the Huincul fault zone is believed to represent its actual northern limit (Gregori *et al.* 2008). Outcrops of Palaeozoic basement rocks in the NPM are scarce and sparsely distributed. Early Cambrian and Mid-Ordovician magmatic rocks crop out in the NE (Pankhurst *et al.* 2006, 2014; Rapalini *et al.* 2013) and were respectively correlated with the Cambrian Pampean (e.g. Rapela *et al.* 1998; Iannizzotto *et al.* 2013) and Ordovician Famatinian (e.g. Pankhurst *et al.* 1998; Dahlquist *et al.* 2008) belts in central and northwestern Argentina. In the western and southwestern margins of the NPM basement rocks of uncertain age were intruded by Devonian granitoids and then early Carboniferous I-type and mid-Carboniferous S-type granites (Pankhurst *et al.* 2006). Permian granites are very extensive and have widespread exposures (Fig. 1, inset A).

The Deseado Massif is located south of the Meso-Cenozoic San Jorge basin (Fig. 1). Palaeozoic basement rocks are poorly exposed and consist of weathered and altered granitoids of Silurian and Devonian age intruding Neoproterozoic metasedimentary rocks (Pankhurst *et al.* 2003). The southern boundary of the Deseado Massif is the Jurassic–Cretaceous Magallanes basin, which extends over most of Tierra del Fuego and the adjoining mainland areas (Fig. 1). Crystalline basement does not crop out there but igneous and metamorphic basement has been recovered from drill cores in which Cambrian foliated peraluminous granitoids are variably transformed to orthogneisses (Sölner *et al.* 2000; Hervé *et al.* 2010).

Two possible Late Palaeozoic magmatic belts

Based on the geographical distribution of late Palaeozoic rocks, and in part K–Ar mica ages for drill core material from the San Jorge basin, Ramos (2008) proposed two separate magmatic arcs (Fig. 1): the partially coeval northern and western belts. This subdivision has been followed in the treatment of data here, partly to test for significant differences between northern and western Permian magmatism. According to Ramos (2008), the northern arc was active before and during the collision of Patagonia with the rest of South America; on the basis of old K–Ar dating of borehole material Ramos projected the western belt across the San Jorge basin to the Deseado Massif, with probable prolongation to the south into the submarine Dungeness High (Fig. 1). The western belt also contains Devonian and mid-Carboniferous igneous rocks and Ramos (2008) speculated that its origin was linked to subduction and subsequent collision of the Antarctic Peninsula. Hervé *et al.* (2010) reported the presence of a Permian metamorphic event in Tierra del Fuego, documented by the development of low Th/U metamorphic zircon. This event affected Cambrian igneous and sedimentary rocks, and was followed by at least 8–12 km of exhumation before Middle Jurassic times. Eroded cover rocks, together with the Permian granitoids of the NPM, have been proposed as the principal sources of Permian detritus for the Late Palaeozoic–Early Mesozoic metasedimentary rocks that crop out widely at the margin of

Patagonia and the Antarctic Peninsula (e.g. Hervé *et al.* 2003, 2010; Pankhurst *et al.* 2006; Fanning *et al.* 2011; Castillo *et al.* 2016).

Permian magmatism in the North Patagonian Massif

The NPM exhibits widespread Permian granitoid magmatism, ranging in age throughout the Permian period and extending into the Triassic (Pankhurst *et al.* 1992, 2006; Chernicoff *et al.* 2013). The composition of these granitoids is variable, including those with metaluminous I-type and peraluminous S-type affinities, intruding Cambrian–Ordovician metamorphic rocks in the northern sector, and Carboniferous metamorphic rocks in the western and southern areas (Llambías & Rapela 1984; Pankhurst *et al.* 2006; López de Luchi & Cerredo 2008; López de Luchi *et al.* 2010). Most of the published U–Pb geochronology for Permian and Triassic intrusions in the NPM are from Pankhurst *et al.* (2006) (see Table 1).

The Laguna del Toro granodiorite and the Piedra del Aguila leucogranite are the oldest Permian intrusions in the western NPM, with Early Permian ages of 294 ± 2 and 290 ± 3 Ma respectively (Table 1); both bodies have been deformed.

In the northeastern corner of the NPM, the oldest Permian granite is the unfoliated Navarrete granite, dated at 281 ± 3 Ma (Table 1). It intrudes late Carboniferous meta-igneous and Cambrian–Early Ordovician metasedimentary rocks (Pankhurst *et al.* 2006; López de Luchi *et al.* 2010). This intrusion was assigned to a subduction regime on the basis of major and trace element data (Rapela & Caminos 1987). Also in the northern part, the La Esperanza plutonic complex includes the unfoliated, high-K, calc-alkaline Prieto granodiorite and Donosa granite (Llambías & Rapela 1984; Martínez Dopico *et al.* 2013). The Prieto granodiorite is the largest and the oldest unit of this complex, dated at 273 ± 2 Ma; it intrudes a sequence of low-grade metasedimentary rocks (Fig. 1, inset A). The last pulse of the magmatism in this area was dominated by the Calvo granite (250 ± 2 Ma), and related acid dykes that represent felsic volcanism of the Dos Lomas complex (Pankhurst *et al.* 2006). The Yaminué complex also occurs in the northern part of the NPM, consisting of foliated granitoids and locally undeformed leucogranitic dykes (López de Luchi *et al.* 2010) dated at around $250–260$ Ma (Chernicoff *et al.* 2013; Pankhurst *et al.* 2014).

Other isolated outcrops of Permian magmatism occur in the NPM and also in the Sierra de la Ventana area, north of the NPM (Fig. 1, inset A). The Boca de la Zanja granodiorite in the southeastern part of the NPM (sample BOZ-1) has a U–Pb zircon age of 257 ± 2 Ma (Pankhurst *et al.* 2006). The López Lecube intrusion (sample SLV-109) consists of syenitic and granitic rocks, isolated from other igneous and sedimentary rocks that crop out in the Sierra de la Ventana area (Gregori *et al.* 2003). It has an age of 258 ± 2 Ma (Pankhurst *et al.* 2006).

Samples and methods

Three new Permian samples come from the deepest parts (1700–2030 m) of drill cores in the Magallanes basin (Fig. 1, inset B). These were analysed for whole-rock geochemistry and zircon U–Pb, O- and Hf-isotopic compositions. Zircon grains were separated using standard crushing, hydraulic, magnetic and heavy liquid procedures and then cast in epoxy mounts with Temora (Black *et al.* 2003, 2004) and FC1 (Paces & Miller 1993) reference zircons. The U–Pb isotopic compositions were measured using SHRIMP II, following standard methods (Williams 1998). Ten other igneous samples from the NPM and one sample from the Sierra de la Ventana area (Fig. 1, inset A) were included for the O- and Hf-isotope study, using Permian zircon grains dated previously by Pankhurst *et al.* (2006, 2014).
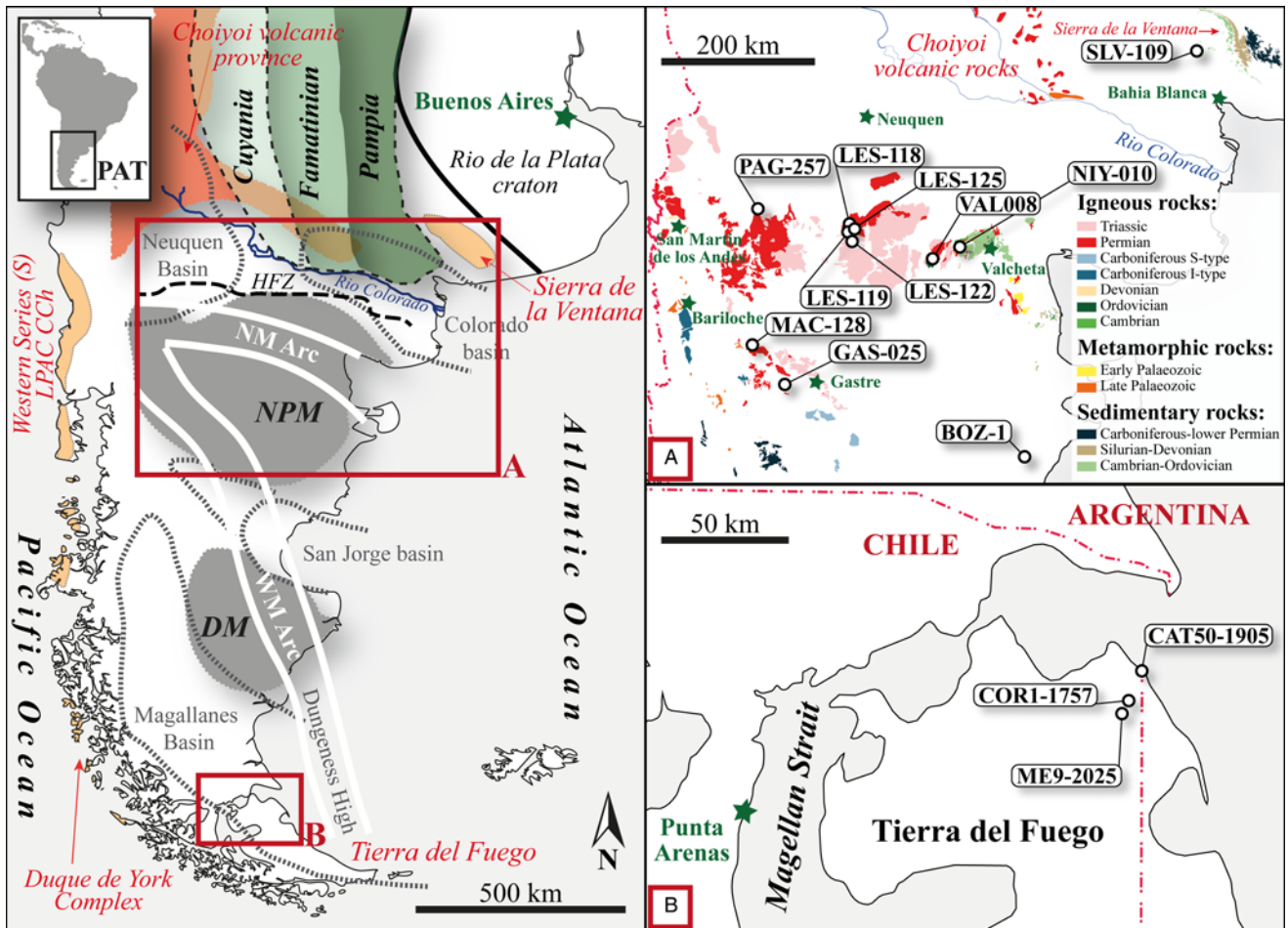
Fig. 1. Sketch map of southern South America showing the studied areas and the main tectonic elements as given in the text. Modified from Pankhurst *et al.* (2014), Choiyoi from Kleiman & Japas (2009), the late Palaeozoic accretionary complex of Central Chile (LPAC CCh) from Hervé *et al.* (2013). NM and WM are the northern and western magmatic arcs (Ramos 2008); HFZ is the Huincul fault zone (Gregori *et al.* 2016). DM, Deseado Massif. Inset A: geological sketch map of the North Patagonian Massif showing the pre-Cretaceous outcrops and sample locations, modified from Pankhurst *et al.* (2006, 2014). Inset B: map of Tierra del Fuego showing the location of the boreholes from which the samples were taken. Please see online version for colour.

After age determination U–Pb analysis pits were removed by light polishing and when necessary samples were recast into megamounts (Ickert *et al.* 2008). O-isotope compositions were measured using SHRIMP II following procedures similar to those described by Ickert *et al.* (2008). The O-isotope ratios and calculated $\delta^{18}O_{VSMOW}$ values were normalized relative to the weighted mean of reference zircon FC1 for the respective analytical session. Hf-isotope compositions were then obtained in the same dated spot by inductively coupled plasma mass spectrometry (ICP-MS) using a Neptune multicollector (MC)-ICP-MS system coupled with a HelEx 193 nm ArF Excimer laser ablation system (Eggins *et al.* 2005). The initial $^{176}Hf/^{177}Hf$ ratios were calculated using the U–Pb crystallization age of each grain or area and results are expressed as initial εHf (εHf$_t$). All measurements were carried out at RSES, The Australian National University. Detailed analytical techniques, corrections and reproducibility of reference zircons are presented in the supplementary material.

Results

A summary of the results is shown in Table 1, with the full analytical datasets given in the supplementary material.

Southern Patagonia

Samples CAT50-1905 and ME9-2025 from Tierra del Fuego are classified as granodiorite, whereas sample COR1-1757 is a metamorphosed granite (detailed description and geochemistry are given in the supplementary material). The morphology of the zircon grains in all samples from Tierra del Fuego is similar; all are considered to be primary igneous crystals mostly medium to coarse (length $100 – 350\,\mu m$), pale pink, euhedral and elongated. Cathodoluminescence (CL) images show internal structures comprising thin oscillatory zoned rims enclosing cores (Fig. 2). The cores form a significant component of each grain, ranging from 80 to 200 μm in length; most are distinguished from their rims by irregular contacts, which truncate the internal zoning. Zoning patterns of cores range from oscillatory to unzoned, and some have outer parts showing a very thin discontinuous layer with bright CL. They are interpreted as being inherited igneous zircons. The analysed rims (between 19 and 21 in each sample) have U and Th concentrations mostly ranging from *c.* 60 to *c.* 650 ppm and from *c.* 50 to *c.* 500 ppm respectively; in all cases the Th/U ratios range from 0.2 to 1.1. The weighted mean $^{206}Pb/^{238}U$ ages for samples COR1-1757, CAT50-1905 and ME9-2025 are 254 ± 3, 254 ± 3 and 258 ± 3 Ma respectively (Fig. 3).

The O- and Hf-isotope zircon compositions for the Tierra del Fuego Permian samples analysed are similar in all samples (Fig. 4). Permian igneous rims yield $\delta^{18}O$ values ranging from 7.3 to 9.2‰ (although sample CAT50-1905 has two grains yielding $\delta^{18}O$ >10‰). There is no significant change in $\delta^{18}O$ from core to rim, with the cores having $\delta^{18}O$ values of 7.0 – 9.1‰. The εHf$_t$ values of the rims range from −8.2 to −3.7: the cores generally have less negative values (−5.3 to +0.5), but they fit a simple crustal evolution

Table 1. *Summary of analysed samples and results*

Sample number	Place name; rock type	Location		Magmatic rims			Inheritance		
		Latitude (°S)	Longitude (°W)	U–Pb age ±2σ (Ma)	δ^{18}O (‰)	Initial εHf	U–Pb age (Ma)	δ^{18}O (‰)	Initial εHf
SLV-109	López Lecube; granite	38.132778	62.708889	258 ± 2*	6.01–7.05	−5.37 to −7.04	–	–	–
LES-118	Calvo; granite	40.329444	68.440000	250 ± 2*	4.39–5.85	−5.56 to −8.97	–	–	–
LES-122	La Esperanza; rhyolite	40.486389	68.432500	246 ± 2*	5.14–6.65	−7.34 to −8.66	–	–	–
LES-125	La Esperanza; felsic dome	40.362222	68.415556	264 ± 2*	6.57–7.55	−3.78 to −11.40	–	–	–
LES-119	Prieto; granodiorite	40.380556	68.458056	273 ± 2*	5.97–7.32	−2.86 to −4.62	–	–	–
NIY-010	Navarrete; granite	40.592500	66.565000	282 ± 3*	4.83–6.46	4.71 to 1.70, −5.05	*c.* 425–630	8.05 (1 grain)	−0.84 (1 grain)
							c. 1050; 1150	6.39 (1 grain)	9.78 (1 grain)
VAL-008	Yaminué; granodiorite	*c.* 40.7800	*c.* 67.1700	251 ± 2†	6.11–7.65	−4.56 to −14.72	–	–	–
PAG-257	Piedra del Águila; granite	40.087222	70.085278	290 ± 3*	7.36–8.40	−3.96 to −5.25	*c.* 880; 1810	–	–
MAC-128	Puesto Quintulepu; granite	41.775833	70.298889	282 ± 2*	6.61–7.16	−2.34 to −5.42	*c.* 745	8.17 (1 grain)	4.56 (1 grain)
							c. 1030	–	–
GAS-025	Laguna del Toro; granodiorite	42.356111	69.863056	294 ± 2*	6.84–7.83	0.10 to −4.38	*c.* 960	6.71 (1 grain)	2.95 (1 grain)
BOZ-1	Boca de la Zanja; granite	43.442222	65.942500	257 ± 2*	6.21–7.68	−5.50 to −7.18	*c.* 510	10.19 (1 grain)	−5.14 (1 grain)
							c. 1030	7.75 (1 grain)	4.40 (1 grain)
CAT50-1905	Tierra del Fuego; granodiorite	52.663641	68.612822	254 ± 3	7.34–12.31	−4.45 to −8.21	*c.* 470	–	–
							c. 520–540	*c.* 8.15 (3 grains)	*c.* −1.95 (3 grains)
							c. 960	–	–
ME9-2025	Tierra del Fuego; granodiorite	52.812583	68.719898	258 ± 3	8.11 to 9.04	−3.66 to −7.28	*c.* 510–660	*c.* 7.99 (2 grains)	*c.* −3.4 (2 grains)
COR1-1757	Tierra del Fuego; Granite	52.782645	68.690408	254 ± 3	7.32 to 8.82	−3.92 to −7.48	*c.* 520–580	*c.* 8.79 (3 grains)	*c.* −0.62 (3 grains)

*Pankhurst *et al.* (2006).
†Pankhurst *et al.* (2014).

P. Castillo *et al.*

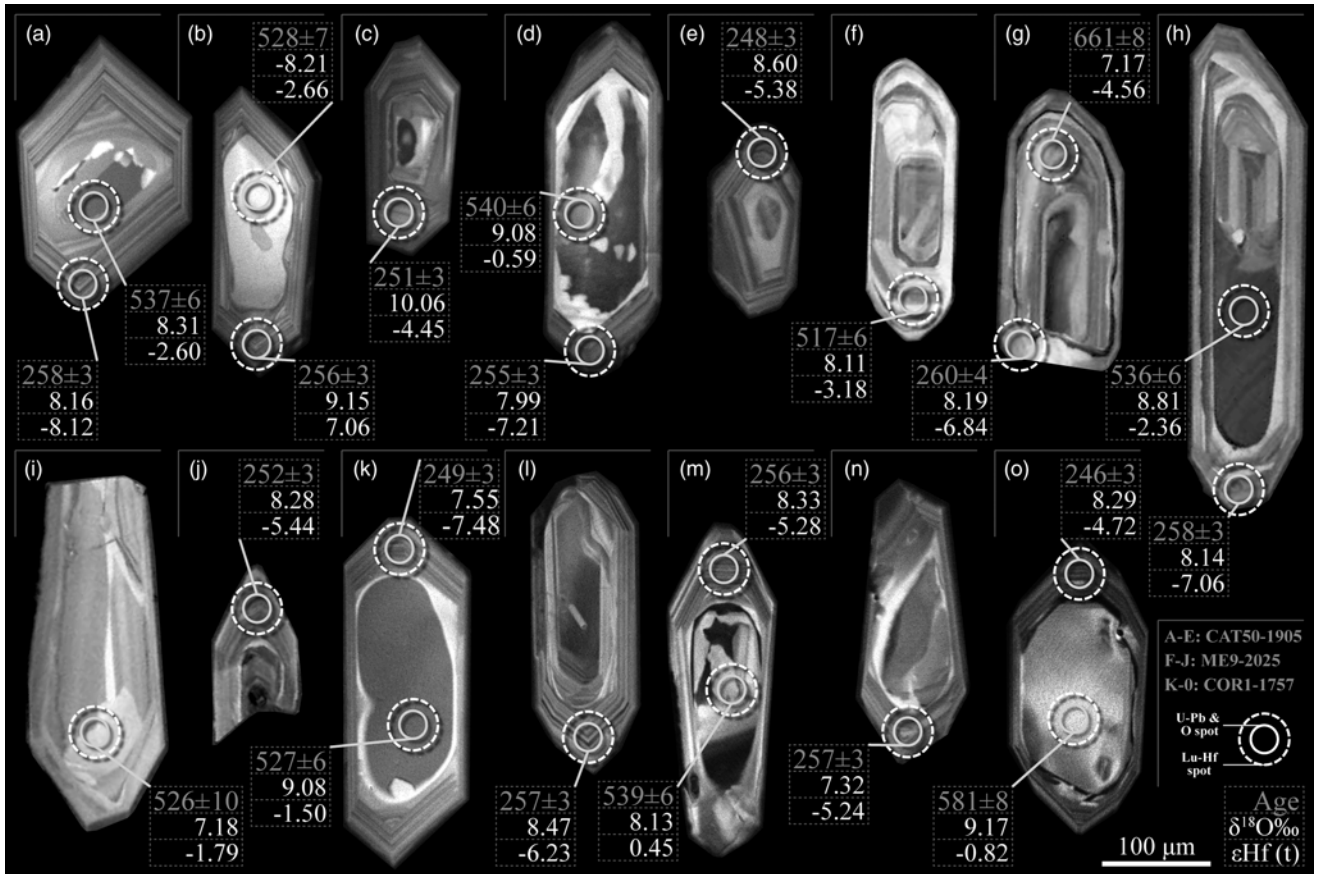**Fig. 2.** Representative CL images of igneous zircons from Tierra del Fuego samples, with U–Pb dates, $\delta^{18}O$ and initial εHf values of each analysed area.

path implying a common source that separated from depleted mantle in Mesoproterozoic times (Fig. 4).

Northern Patagonia

Zircons from samples located in the western part of the NPM, MAC-128 (281 ± 2 Ma), GAS-025 (294 ± 2 Ma) and PAG-257 (290 ± 3 Ma), have similar $\delta^{18}O$ values ranging from 6.7 to 8.4‰ and εHf_t ranging from +0.1 to −5.4 (Fig. 5). All these samples have older inherited cores, with similar or higher $\delta^{18}O$, from 6.7 to 8.2‰, and positive εHf_t ranging from +4.6 to +3.0 (Table 1).

The zircon rims in the 281 ± 3 Ma granite sample NIY-010 (Navarrete granite) are distinguished by low $\delta^{18}O$ of 4.8 – 6.5‰ and mostly positive εHf_t values (Fig. 5). Whereas the zircon rims have juvenile or mantle-like O-isotope signatures, the inherited Cambrian and Mesoproterozoic cores (as dated by Pankhurst et al. 2006) have higher $\delta^{18}O$ values (Table 1).

Igneous zircons in the Yaminué complex sample (VAL008) show a range of $\delta^{18}O$ from 6.1 to 7.7‰, similar to that recorded by zircon in sample VAL009 previously reported by Pankhurst et al. (2014). εHf_t values are more variable than those from sample VAL009, ranging from −4.6 to −14.7 (Fig. 5).

Magmatic rocks from the La Esperanza area (samples LES-118, -119, -122 and -125) show a wide range of zircon O- and Hf-isotope compositions (Fig. 5). The Prieto granodiorite, sample LES-119 (273 ± 2 Ma), has zircon $\delta^{18}O$ values from 6.0 to 7.3‰ and negative εHf_t values ranging from −2.9 to −4.6. Zircon in the 264 ± 2 Ma rhyolite sample (LES-125) shows similar $\delta^{18}O$ values from 6.6 to 7.6‰, but more negative εHf_t values, ranging from −3.8 to −14.4 In contrast, the Early Triassic samples (sample LES-118 and LES-122) have zircons with negative εHf_t of −5.6 to −9.0, but $\delta^{18}O$ values from 4.4 to 6.7‰, within the range of mantle-derived zircon.

In the Sierra de la Ventana area, igneous zircons from the López Lecube syenite sample SLV-109 (258 ± 2 Ma) have negative εHf_t values between −5.4 and −7.0, with $\delta^{18}O$ ranging from 6.0 to 7.1‰. These results are comparable with those for sample BOZ-1 (257 ± 2 Ma) from the SE NPM, between the two arcs proposed by Ramos (2008). However, sample BOZ-1 has older inherited zircon components with higher $\delta^{18}O$ values than the magmatic Permian rims (Table 1).

Discussion

The isotopic trends of the Permian magmatic rocks

Northern Patagonia

A major metasedimentary input is recorded for magmas generated in the western part of the NPM (samples MAC-128, GAS-025 and PAG-257; Fig. 5), which is consistent with the predominant peraluminous chemistry of rocks in this area (Fig. 6b), although it should be noted that MAC-128 and GAS-025 are themselves metaluminous. In sample MAC-128, the $\delta^{18}O$ values of detrital zircon cores exceed those in equilibrium with mantle or juvenile lower crust and are higher than in the Permian magmatic rims (Table 1). This implies inclusion of crustal material in a slightly more juvenile magma and is consistent with generation in a subduction-related tectonic setting, as previously suggested by the whole-rock geochemistry (Fig. 6; López de Luchi & Cerredo 2008). The O–Hf isotopic compositions in zircons of these samples are similar to those of the subduction-related Permian rocks of the western Chile margin (Fig. 5), suggesting similar tectonic processes.

The zircon O–Hf isotopic compositions of samples from the northern NPM show striking trends when plotted as a function of crystallization age (Fig. 5). Zircon $\delta^{18}O$ values change from mantle-
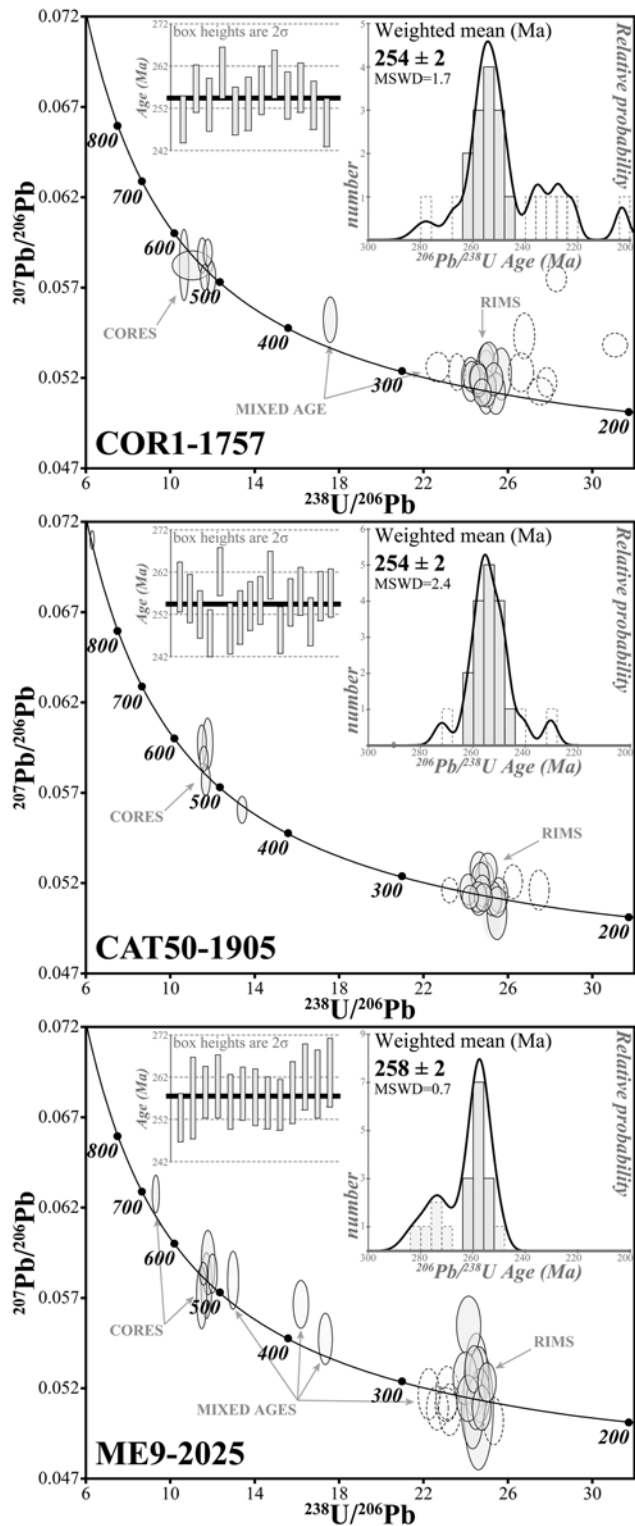
Fig. 3. New SHRIMP U–Pb data for samples from Tierra del Fuego in a Tera–Wasserburg concordia plot; probability density plots of $^{206}Pb/^{238}U$ ages with stacked histograms are also shown; error ellipses are at the 2σ level. Location of samples is shown in Figure 1. Weighted mean $^{206}Pb/^{238}U$ ages are given for the magmatic rims and are considered the best estimates for the igneous crystallization age.

Fig. 4. U–Pb zircon ages ($^{206}Pb/^{238}U$) v. initial εHf and δ^{18}O values for zircons analysed in this study for samples from Tierra del Fuego. Error bars are at the 2σ level, although it should be noted that most of these are smaller than the actual symbols. The value for zircon with mantle δ^{18}O is from Valley *et al.* (2005). Dotted lines connect cores and rims of each zircon.

The O–Hf isotopic compositions of magmatic zircons from the Navarrete granite indicate that it crystallized from a juvenile magma, within the accepted δ^{18}O range for zircon with mantle-like compositions. However, the εHf$_t$ values (<+5) are lower than those of contemporaneous depleted mantle (about +15) and are in keeping with a significant time since separation (Hf depleted-mantle model ages are *c.* 1100 Ma). The unradiogenic Hf was either inherited directly from a Mesoproterozoic lower crustal source or resulted from contamination with such lower levels of the crust. The contrasting more crustal compositions of the inherited cores suggest that, even though the juvenile magma interacted with ^{18}O-richer upper crustal material, there was not complete equilibration.

The combined O–Hf isotopic compositions of zircons from La Esperanza (samples LES-118, -119, -122, and -125) indicate highly evolved sources, but different degrees of assimilation of ^{18}O-rich upper crustal material, as is recorded by the negative older crust-like εHf$_t$ but contrasting δ^{18}O values (Fig. 5). Therefore, the δ^{18}O–εHf$_t$ inter-pluton trend for these samples can be characterized by variations in the degree of ^{18}O enrichment (Fig. 7a) and may indicate melting of different levels of an early Mesoproterozoic crust (*c.* 1600 Ma). Lower crust or enriched lithosphere igneous sources indicated by negative εHf$_t$ but mantle-like δ^{18}O in zircon at the Permo-Triassic boundary interval may indicate a change in geodynamic conditions at this time.

The O-isotope compositions of zircons from the Calvo granite and La Esperanza rhyolite (Fig. 5) suggest magmas derived from the mantle, but the time-dependent Hf-isotope compositions point to magmas derived from evolved, unradiogenic crustal sources. This

like for the Permian Navarrete granite, through more sediment-like values for the Yaminué and Prieto granodiorites, and returning to mantle-like values for the early Triassic zircons from the Calvo granite and La Esperanza rhyolite (Fig. 5). This trend is to some extent mirrored by the zircon εHf$_t$ values, although the Calvo granite and La Esperanza rhyolite have negative εHf$_t$, not the expected positive values.
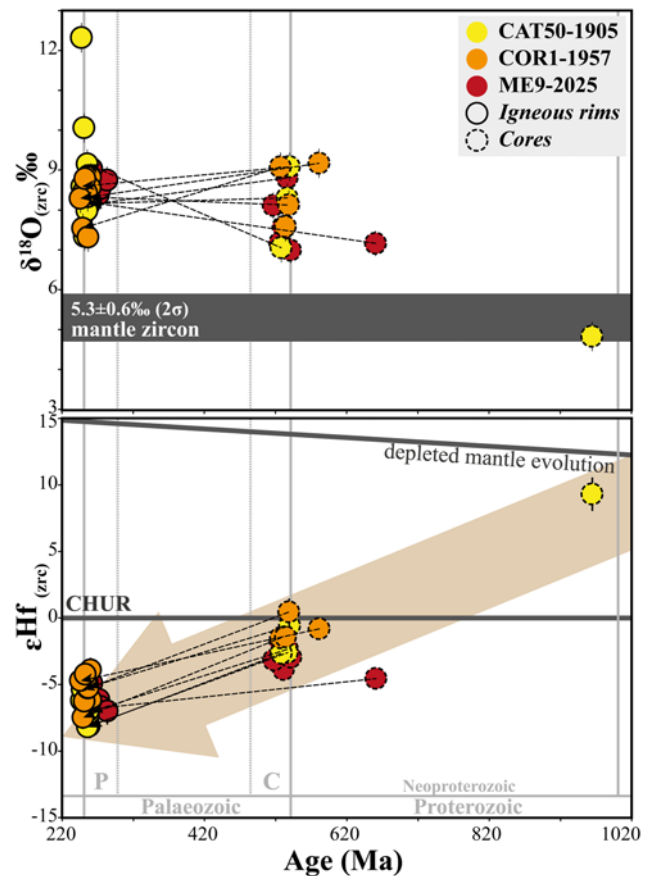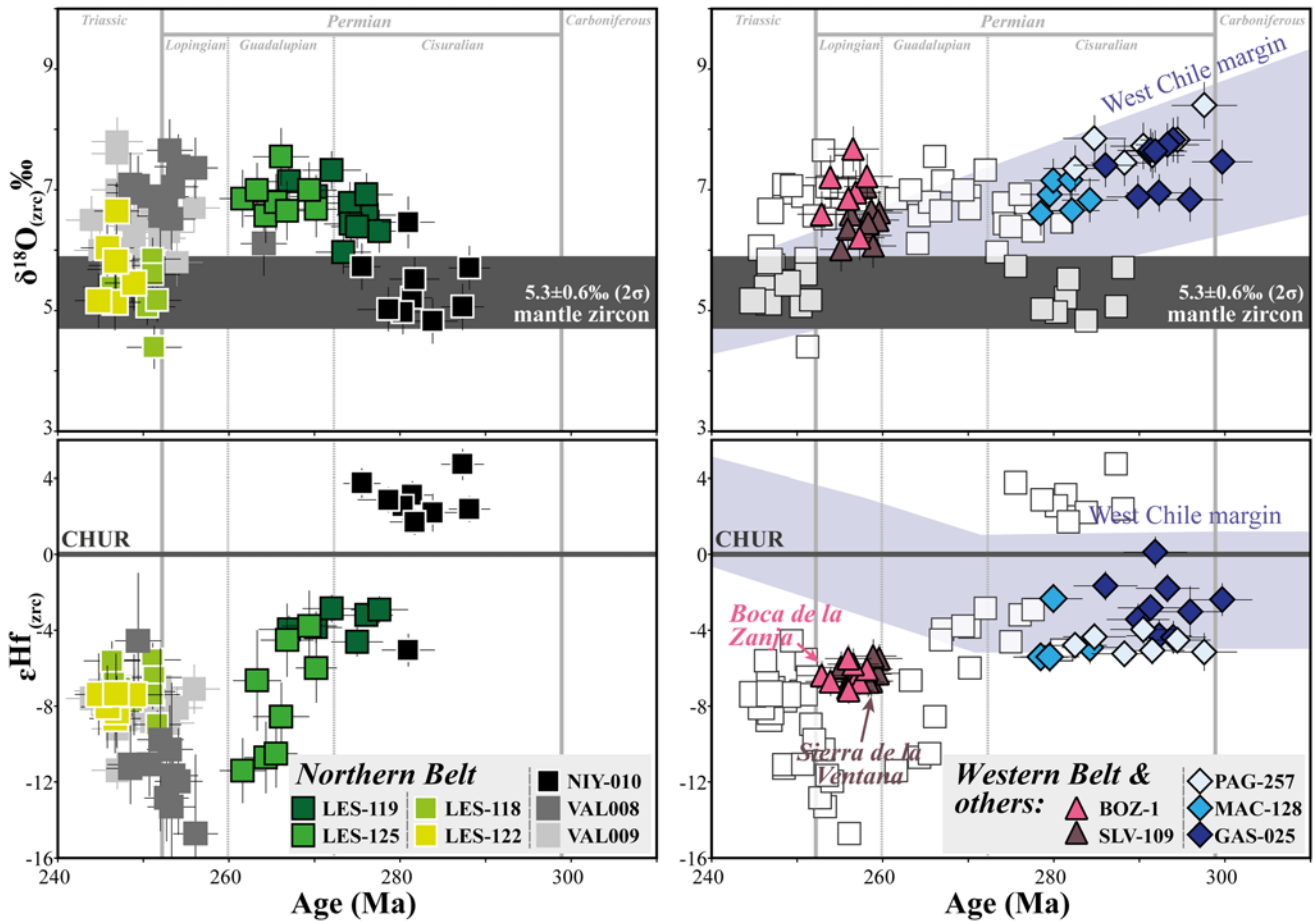
Fig. 5. U–Pb zircon ages ($^{206}Pb/^{238}U$) v. initial εHf and $\delta^{18}O$ values for zircons analysed in this study for samples from the North Patagonian Massif. Error bars are shown at the 2σ level. The value for zircon with mantle $\delta^{18}O$ is from Valley *et al.* (2005). Light grey fields represent the range of Permian–Triassic magmatism in the western Chile margin, from Deckart *et al.* (2014), Hervé *et al.* (2014) and del Rey *et al.* (2016). The O–Hf data for sample VAL009 are from Pankhurst *et al.* (2014).

implies that the source was separated from the depleted mantle for some considerable time prior to magma genesis (Hf depleted mantle model ages of 1500 – 1700 Ma) but without recycled intra-crustal additions, as the zircon $\delta^{18}O$ values remain approximately constant. The $\delta^{18}O$ composition in these zircons would thus be indistinguishable from those derived from primitive mantle magmas or lower crustal source regions. Thus, the importance of combining the O isotopic system with a time-dependent one as provided by the Lu–Hf system is clear from this study. It underlines the limitations in using Hf model ages to determine timing of juvenile magmas additions to the continental crust (e.g. Nebel *et al.* 2011; Payne *et al.* 2016; Vervoort & Kemp 2016). It has been proposed that mantle-like $\delta^{18}O$ values should be used as a filter for assessing whether zircon Hf model ages have some geological meaning or not (e.g. Dhuime *et al.* 2012). However, tracking additions of juvenile components to a mantle-like O and negative εHf$_t$ is difficult to assess using just those isotopic systems and therefore Hf model ages would remain of doubtful geological significance. This is especially a problem in extensional continental settings, where there can be significant melting of the crust, including lower crustal material.

It has been shown that isotope–time trends may correlate with the patterns of compressional and extensional events, as juvenile magmatic input can be enhanced during extension (Kemp *et al.* 2009). A change from a convergent plate margin to an extensional regime is recorded in the San Rafael Massif during the emplacement of the Permian Choiyoi Group at *c.* 265 Ma (Kleiman & Japas 2009). The same change may have occurred in the NPM, although it would have been contemporaneous with a compressional setting in

the Sierra de la Ventana and Yaminué complex (Kleiman & Japas 2009; López de Luchi *et al.* 2010). The change in zircon O–Hf isotopic composition of granite samples VAL-008 and VAL-009 from the Yaminué complex (Figs 5 and 7a), may also define an inter-pluton trend towards more juvenile isotopic compositions indicating increasing involvement of a mantle-like source around 250 Ma. Mixing is also recorded in the SE NPM at *c.* 255 Ma, where zircons from sample BOZ-1 show a decrease of $\delta^{18}O$ values from core to rim indicating mixing of a lower crust or enriched lithosphere source with ^{18}O-rich upper crustal material, perhaps by entrainment of old crustal zircons. Similar O–Hf isotopic compositions in zircons of the contemporaneous sample SLV-109 (Fig. 7b) in the Sierra de la Ventana suggest melting and recycling of similar Mesoproterozoic crustal material.

Pankhurst *et al.* (2014) suggested a complex but essentially Mesoproterozoic source for Permian granites in the Yaminué complex. The apparent εHf$_t$–$\delta^{18}O$ trend for sample VAL-009, and perhaps also for sample LES-125, indicates the need for a less radiogenic source (Fig. 7a). Chernicoff *et al.* (2013) produced evidence of significant Archaean inheritance in a 260 Ma granite from the Yaminué complex and calculated Hf model ages in the range 1900 – 3300 Ma. However, only zircons with mantle-like O isotopic composition can be considered to provide reliable Hf model ages (Dhuime *et al.* 2012) and those with more ^{18}O-enriched isotope compositions reflect crustal reworking and provide only mixed model ages. Thus the data can also be interpreted as due to mantle-derived magmas reworking metasedimentary protoliths containing a high proportion of Archaean detritus (Fig. 7a).
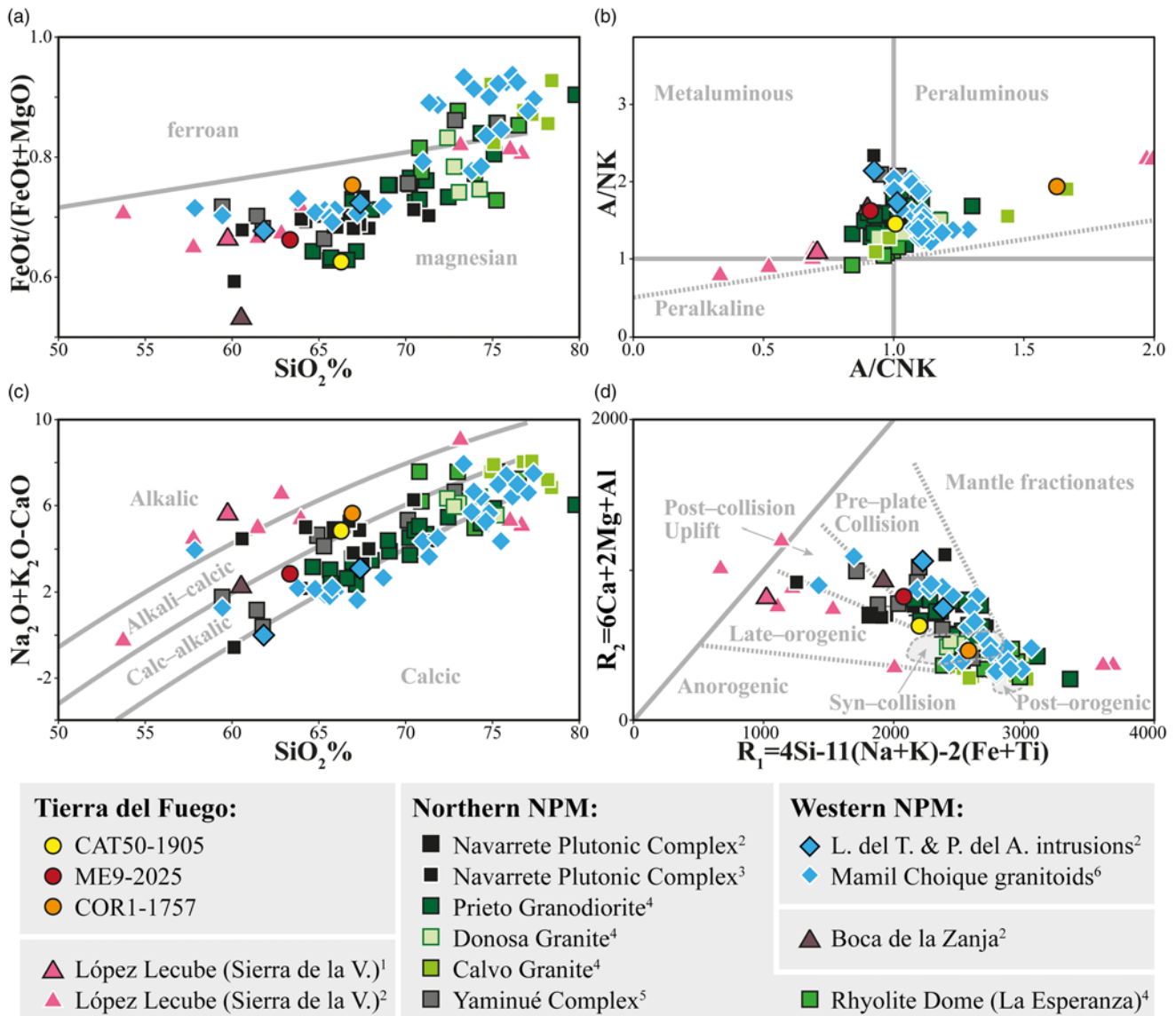
Fig. 6. Major element geochemical trends in the Permian and early Triassic units discussed in this study. (**a**) Variation of FeOt/(FeOt + MgO) v. SiO$_2$. After Frost *et al.* (2001). (**b**) A/CNK v. A/NK diagram after Maniar & Piccoli (1989). A, Al$_2$O$_3$; N, Na$_2$O; K, K$_2$O; C, CaO, all in molar proportions. (**c**) Modified alkali–lime diagram (Frost *et al.* 2001). (**d**) R$_1$ v. R$_2$ multi-cationic discrimination diagram after Batchelor & Bowden (1985). Data for the North Patagonian Massif were taken from (1) Gregori *et al.* (2003), (2) Pankhurst *et al.* (2006), (3) Rapela & Caminos (1987), (4) Rapela & Llambias (1985), (5) Pankhurst *et al.* (2014) and (6) López de Luchi & Cerredo (2008).

Southern Patagonia

Our SHRIMP U–Pb zircon age data record the first evidence of late Permian magmatism in southernmost Patagonia. The igneous zircon rims have O–Hf isotopic compositions that indicate that the magma source had a strong supracrustal influence and involved recycling of ^{18}O-richer Cambrian upper crustal material (Fig. 4). Sample CAT50-1905 has some zircon areas with an even stronger supracrustal influence, also with Tonian and Cambrian inheritance. This suggests the presence of a metasedimentary influence in the source region, as shown in Figure 6b. Our data are consistent with felsic, crust-derived, late Permian magmatism, and indicate correlations with other events in northern Patagonia. As shown in Figure 7b, the apparent εHf$_t$–δ^{18}O trend for Tierra del Fuego samples is similar to that proposed for the NPM.

A Permian metamorphic event in Tierra del Fuego at upper amphibolite to granulite metamorphic facies has been dated at 267 ± 3 Ma (U–Pb SHRIMP zircon ages, Hervé *et al.* 2010). If the magmatism and metamorphism are related, then samples analysed in this study record post-orogenic magmatism that could be associated with extensional collapse and partial melting of upper

crust related to thermal relaxation and/or exhumation of the orogen. Ramos (2008) suggested extensional collapse in the hanging wall during the Permian (e.g. for initiation of the La Golondrina basin) after the hypothetical collision of the Antarctic Peninsula with Patagonia. However, the contemporaneous occurrence of mid- to late Permian magmatism and metamorphism in Tierra del Fuego and the Antarctic Peninsula (Millar *et al.* 2002; Riley *et al.* 2012) indicates that pre-collisional subduction could not have been located between the two areas. It is more likely that Permian east-directed subduction was active along a joint Patagonia–Antarctic Peninsula margin (e.g. Castillo *et al.* 2016).

Northern Patagonia: autochthonism versus collisional deformation

Continuity of the NPM crust with South America in the early Palaeozoic is suggested by several lines of evidence: the apparent continuation of Cambrian (Pampean) and Ordovician (Famatinian) orogenic belts, and similar age patterns of detrital zircons from Cambro-Ordovician metasedimentary rocks (Pankhurst *et al.* 2006,
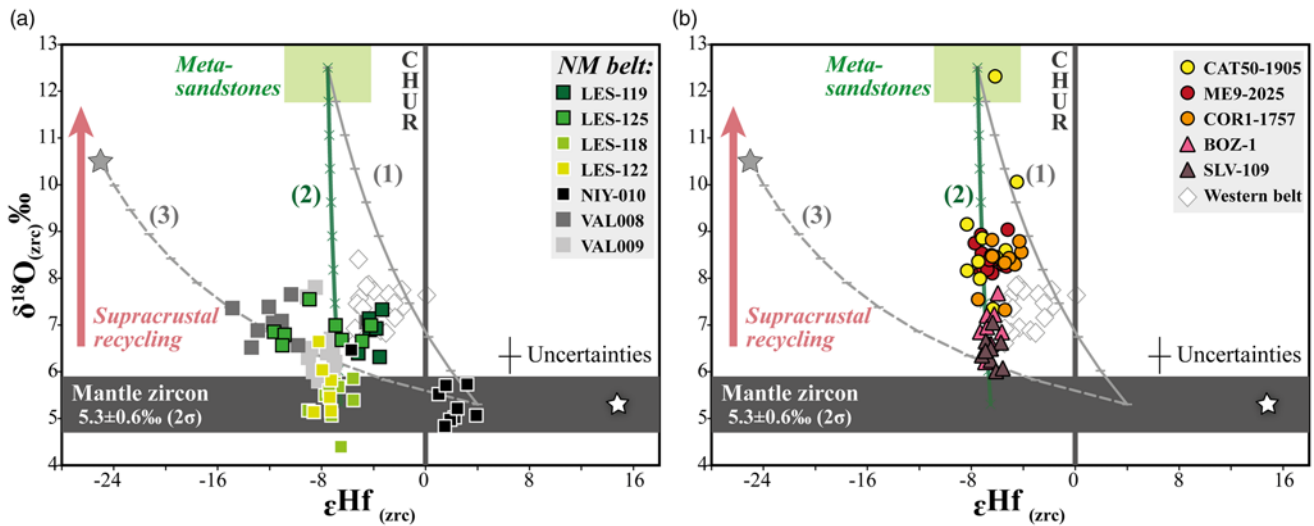
Fig. 7. Plot showing εHf_t v. δ^{18}O values in zircon from the northern NPM (**a**), Sierra de la Ventana, Boca de la Zanja and Tierra del Fuego (**b**) with the estimated compositions of potential end members and theoretical mixing trends. The Palaeozoic metasedimentary country rocks are the Coli Niyeu (Labudía & Bjerg 1995) and Nahuel Niyeu formations (Chernicoff & Caminos 1996). No Hf- or O-isotope data are available, but εHf_t was estimated from the whole-rock Nd-isotope composition of the Nahuel Niyeu Formation (Pankhurst *et al.* 2006), using the Nd–Hf correlation of Vervoort *et al.* (1999) and δ^{18}O values between 10 and 30‰ were assumed as typical of sedimentary rocks. The isotopic compositions of the end members were as follows. (1) δ^{18}O = 5.3‰ and εHf_t = 4 for the juvenile material, taken from the Navarrete granite, and δ^{18}O = 12.5‰ and εHf_t = −7.5, estimated for the Nahuel Niyeu Formation. The juvenile/supracrustal ratio of Hf concentrations was taken as 0.5. (2) δ^{18}O = 5.3‰ and εHf_t = −6.5 for the juvenile lower crust, taken from the Calvo granite. The relative Hf concentrations are the same as in model 1. (3) Hypothetical components to show the need for a less radiogenic supracrustal component. Values for the juvenile component are as in model 1, the hypothetical supracrustal component (grey star) has δ^{18}O = 10.5‰, εHf_t = −26 and the juvenile/supracrustal ratio of Hf concentrations is 0.3. For all models, the value of D_{Hf} = 1 and all εHf_t values have been recalculated to t = 250 Ma. Depleted Mantle (white star) values are from Vervoort & Blichert-Toft (1999) and the mantle δ^{18}O is from Valley *et al.* (2005).

2014; Rapalini *et al.* 2013). However, deformation in the Sierra de la Ventana has been interpreted as evidence of a collisional setting (e.g. Ramos 1984, 2008; Kay *et al.* 1989; von Gosen 2003; Ramos *et al.* 2014). Synorogenic tuff deposits of the Tunas Formation in the Sierra de la Ventana, dated as middle Early Permian at 280.8 ± 1.9 Ma (López-Gamundí *et al.* 2013) and 282.4 ± 2.8 Ma (Tohver *et al.* 2008), are contemporaneous with the emplacement of the Navarrete granite. However, the emplacement of this granite seems to preclude a collisional setting as it is unfoliated and has juvenile isotopic characteristics.

In the Sierra de la Ventana, a second deformation event occurred in the late Permian based on ^{40}Ar/^{39}Ar ages from biotite, muscovite and sericite of 265 – 260 Ma (Tohver *et al.* 2008), in the same time interval that has been assigned to collision in the northeastern NPM. This deformation is recorded in the Yaminué complex (López de Luchi *et al.* 2010), dated at *c.* 260 – 250 Ma (Chernicoff *et al.* 2013; Pankhurst *et al.* 2014). If the collision occurred during the second pulse of deformation, then the Navarrete granite may have formed as a consequence of pre-collisional subduction. However, there is no evidence for widespread or prolonged pre-Permian subduction-related magmatism in the NPM that would support the idea of an approaching allochthonous terrane, for example, throughout Carboniferous time. Ramos *et al.* (2014) reported εHf_t values ranging between +10.5 and −1.9 for Late Carboniferous–Early Permian detrital zircons from the Tunas Formation, which they ascribed to relatively juvenile sources in the northern NPM implying close proximity of the two areas.

In the western part of the NPM, Early Permian and Carboniferous magmatism (I-type and S-type) can be seen as a continuation of the Late Carboniferous–Early Permian subduction-related magmatism recorded all along the western continental margin; that is, in the Chilean Precordillera (Munizaga *et al.* 2008; Maksaev *et al.* 2014, and references therein), the southern extension of the Frontal Cordillera (27 – 31°S, Hervé *et al.* 2014; del Rey *et al.* 2016, and references therein), and the Cordillera del Viento in Argentina (37°S, Llambías *et al.* 2007). The zircon O–Hf isotopic data for late

Palaeozoic–Triassic granites in the western Chile margin show evolution from crust-derived magmas during the Early Permian magmatic arc phase to more juvenile compositions during the Late Permian–Triassic (Hervé *et al.* 2014; del Rey *et al.* 2016). This is the reverse of the trend of Permian magmatism in the northern NPM, but similar to the O–Hf isotopic compositions in zircons of the western NPM (Fig. 5). A sample from the Huingancó complex in the Cordillera del Viento (Hervé *et al.* 2013) is plotted in Figure 8 as a reference. Early stages of Choiyoi magmatism dated at *c.* 281 Ma (Rocha-Campos *et al.* 2011) are also attributed to an active continental margin, with the later stages following post-orogenic collapse and extension (Kleiman & Japas 2009). This indicates similar tectonic processes north of, and continuing into, the western NPM during Early Permian times.

These similarities suggest continuity of the NPM with South America during the late Palaeozoic and the observed deformation would be equally explicable without the closure of an ocean between them, as previously maintained by other researchers (Gregori *et al.* 2008, 2016; Pankhurst *et al.* 2014). Kleiman & Japas (2009) proposed continental blocks that rotated in a clockwise manner, in relation to a curved margin, to explain contemporaneous extensional and compressional settings in the San Rafael Massif and Sierra de la Ventana, respectively. Granitic intrusions in coevally extensional and contractional domains have also been reported, by Gregori *et al.* (2016), in the NPM in the late Permian. Those researchers proposed an indentation-escape tectonic model (Gregori *et al.* 2008) and curvilinear regional lineaments dominated by strike-slip movements forming extensional and contractional domains.

Permian igneous and detrital zircons: correlation with the Antarctic Peninsula

The Western Series of the Late Palaeozoic accretionary complex of central Chile crops out directly to the west of the present-day NPM (Willner *et al.* 2004; Hervé *et al.* 2013; Fig. 1). This fossil subduction complex has U–Pb detrital zircon patterns with
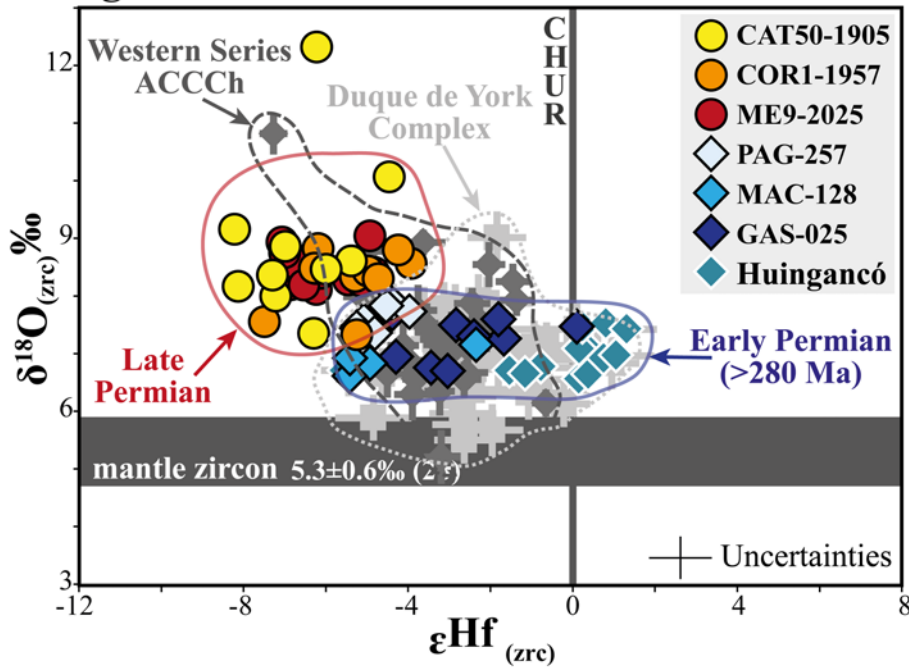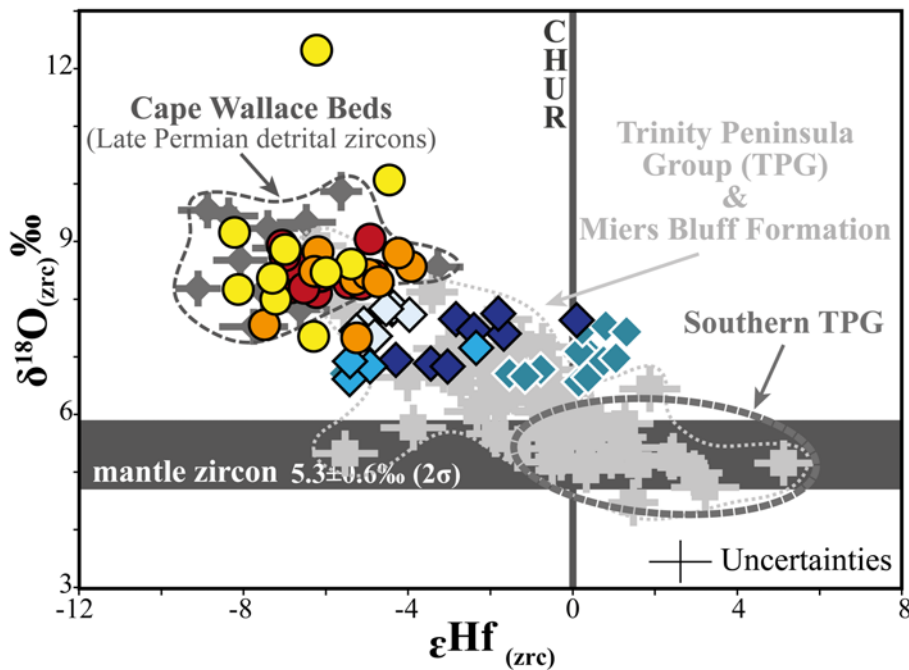
Fig. 8. Variations of εHf$_t$ v. δ^{18}O values in zircon for Permian and early Triassic zircons of samples from Tierra del Fuego and western North Patagonian Massif. The εHf$_t$ v. δ^{18}O values for the Huingancó complex are plotted in the figure for comparison; data from Hervé *et al.* (2013). εHf$_t$ v. δ^{18}O values for Permian and early Triassic detrital zircons from accretionary complexes from Patagonia (above) and the Antarctic Peninsula (below); data for the Western Series of the late Palaeozoic accretionary complex from central Chile (Western Series ACCCh) were taken from Hervé *et al.* (2013), and data for the Duque de York Complex, the Trinity Peninsula Group, Miers Bluff Formation and Cape Wallace beds were taken from Castillo *et al.* (2016).

predominantly Permian and subsidiary Cambrian and Devonian age components (Hervé *et al.* 2013). The similar O–Hf isotopic compositions of detrital Permian zircons (data taken from Hervé *et al.* 2013; Fig. 8), together with similar age components, clearly indicate sources located in the western NPM. South of 46°S (west and south of the Deseado Massif) sediments from the Eastern Andes Metamorphic Complex (Fig. 1) record a change in provenance, with Devonian to late Carboniferous detrital zircon derived from Devonian to Mesoproterozoic sources, and Permian and Triassic zircon derived from Permian sources (Hervé *et al.* 2003; Augustsson *et al.* 2006). The Permian and Triassic metasedimentary complexes in this area, which include the Permian part of the Eastern Andes Metamorphic Complex and the Duque de York Complex (Fig. 1), were supplied with detritus from local Patagonia and West Antarctic sources (Augustsson *et al.* 2006; Castillo *et al.* 2016) and have Permian detrital zircons with O–Hf

isotopic characteristics similar to the Permian igneous rocks of the western NPM (Fig. 8).

Detrital zircons with the characteristics of those from the Tierra del Fuego Permian rocks (i.e. Permian rims and Cambrian cores) have not yet been reported in the southern Patagonian accretionary complexes (Fig. 8). However, the Middle Jurassic Cape Wallace Beds of the northern Antarctic Peninsula have late Permian detrital zircons with strong internal structure, age and isotopic similarities to those in the Tierra del Fuego rocks (Fig. 8). They have the same core–rim structures, U–Pb ages and O–Hf zircon isotopic signatures (Castillo *et al.* 2016). This strongly supports a southern Patagonia–Antarctic Peninsula connection during the Jurassic before the break-up of Gondwana (Lawver *et al.* 1998; Ghidella *et al.* 2002; König & Jokat 2006). Permian and Triassic metasedimentary rocks of the Trinity Peninsula Group in the Antarctic Peninsula, which are correlated with those of the Duque de York Complex in Patagonia,

have Permian detrital zircons with a probable local Permian magmatic arc source (Castillo *et al.* 2015, 2016). The northern Trinity Peninsula Group detrital zircons have comparable O–Hf isotopic signatures to Permian magmatic rocks in the NPM, but the additional southern, more juvenile Permian component has not yet been recorded in southern Patagonia (Fig. 8) and is probably located in West Antarctica (Castillo *et al.* 2016).

Palaeozoic basement rocks of the Antarctic Peninsula include Ordovician-age protoliths, reworked and melted during the Permian, and discrete Silurian, Devonian and Carboniferous magmatic rocks (Millar *et al.* 2002; Riley *et al.* 2012). All these events have been recognized in the evolution of Patagonia, especially in the NPM, where the most geochronological data are available. Furthermore, Permian magmatism and metamorphism at *c.* 275 and *c.* 255 Ma in the north and central Antarctic Peninsula (Millar *et al.* 2002; Riley *et al.* 2012) record similar and contemporaneous processes affecting both southern Patagonia and the Antarctic Peninsula. However, these processes affected different rocks, Cambrian in southern Patagonia and Ordovician in the Antarctic Peninsula. If the Antarctic Peninsula was located west of southern Patagonia, this implies Ordovician crust west of Cambrian crust (basement of Tierra del Fuego), in the same way as the relationship between the Pampean and Famatinian belts north of Patagonia. Thus these regions would have been contiguous not only in the Jurassic but also during the majority of Palaeozoic time. The opposite sense of relationship between the Pampean and Famatinian belts in the NPM may be solved by a curved continental margin in NE Patagonia as proposed by Rapalini *et al.* (2013). A curved continental margin during the Permian, south of 34°S, was also proposed by Kleiman & Japas (2009).

Final considerations: the Gondwanide fold belt

The Sierra de la Ventana formed part of a continuous fold belt along the Gondwana margin known as the Gondwanide fold belt (Du Toit 1937). The sections comprising the Sierra de la Ventana, the Cape
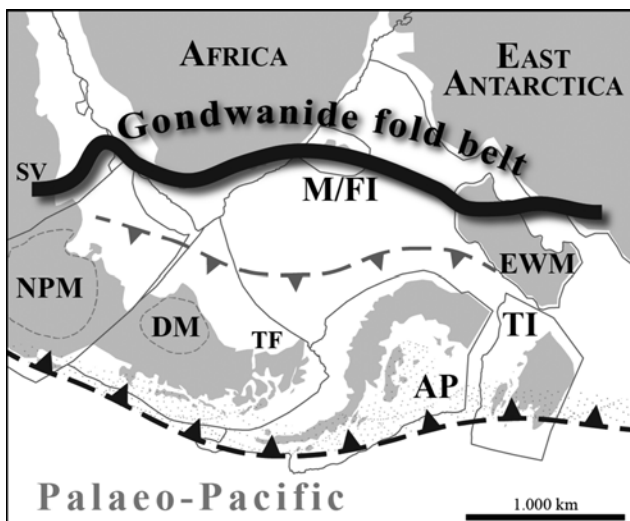

Fig. 9. Schematic reconstruction of SW Gondwana showing Permian plate configuration, and early Permian subduction between South America–Patagonia–Antarctica and the South Africa–Ellsworth sector that resulted in a collision and deformation of the Gondwanide fold belt. The consumed Palaeozoic ocean floor was probably formed in the Cambrian, during the continental rifting that is recorded in the Sierra de la Ventana–Ellsworth sector. AP, Antarctic Peninsula; DM, Deseado Massif; EWM, Ellsworth–Whitmore Mountains block; M/FI , Malvinas/Falkland Islands; NPM, North Patagonian Massif; SV, Sierra de la Ventana; TF, Tierra del Fuego; TI, Thurston Island.

Fold Belt in South Africa, the Falkland/Malvinas Islands and the Ellsworth Mountains (Fig. 9) share similar characteristics: Cambrian sedimentation in a continental rift setting, a Late Cambrian(?) to Carboniferous passive margin and Permian deformation (Curtis 2001; Rapela *et al.* 2003). The deformation occurred up to *c.* 1500 km inland of the previous continental margin and two main hypotheses about its formation have been suggested: collision of an exotic terrane (e.g. Pankhurst *et al.* 2006; Ramos 2008) and flat-slab subduction (Dalziel *et al.* 2000). According to the latter model, the flat slab would involve a non-magmatic zone or a reduction of arc volcanism during the 270–240 Ma interval (Dalziel *et al.* 2013), which is not consistent with the Permian magmatism in the NPM, Tierra del Fuego and the Antarctic Peninsula.

In the case of the collision models, Patagonia has been the preferred candidate for the exotic terrane. Based on reports of the Early Cambrian archaeocyath fauna in the NPM (González *et al.* 2011), resembling taxa in the Transantarctic Mountains in East Antarctica, Ramos & Naipauer (2014) proposed that Patagonia originated as the conjugate margin of the Transantarctic Mountains from Southern Victoria Land to the Pensacola Mountains. This model implies parallel translation of more than 2500 km and does not take into account other tectonic blocks of West Antarctica and their potential correlation with Patagonia and the Transantarctic Mountains. Nor does it consider the absence of Palaeozoic rift-related magmatism in the Transantarctic Mountains. Archaeocyaths also occur in the Ellsworth Mountains, both *in situ* (Henderson *et al.* 1992) and also in Late Carboniferous–Early Permian diamictites (Debrenne 1992). They are in fact widespread, being found in diamictites in the Falkland/Malvinas Islands, South Africa and South America (Stone & Thomson 2005; Stone *et al.* 2012; González *et al.* 2013). This suggests correlations between these glacial deposits during the Late Carboniferous–Early Permian, and supports an extensive early Cambrian reef system (Dalziel *et al.* 2013) as a better explanation for the occurrence of this faunal record. All evidence is consistent with a parautochthonous origin for the NPM (Rapalini 2005; Rapalini *et al.* 2013), as well for the southern part of Patagonia and the Antarctic Peninsula.

Recent studies, based on Re–Os isotopes, suggest lithospheric connections between the Deseado Massif and the Namaqua–Natal belt of South Africa (Mundl *et al.* 2015) or the Falkland/Malvinas block (Schilling *et al.* 2008). Mundl *et al.* (2015) suggested that the formation ages of subcontinental lithospheric mantle domains under southern Patagonia indicate a common origin with crustal sections in the Shackleton Range. It is possible that Patagonia, together with a proto-Antarctic Peninsula, could have rifted partially from the Sierra de la Ventana–South Africa–Ellsworth Mountains sector of west Gondwana during the Cambrian (Rapela *et al.* 2003), to then collide during the Permian (Fig. 9). If this was the case, the northern NPM would not necessarily have rifted completely from South America, and west-directed subduction in the Patagonia–Antarctic Peninsula margin could have continued during Ordovician, Devonian and Early Permian times. In this context, the deformation and magmatism in the northern NPM could be related to west–east-directed compression owing to the indentation of blocks farther east as proposed by Gregori *et al.* (2016).

The possibility of a Palaeozoic ocean basin between Patagonia–Antarctica and the South Africa–Ellsworth sector would imply that ocean floor was consumed. The lack of Palaeozoic magmatic events younger than *c.* 500 Ma in southern Africa, the Falkland/Malvinas Islands or the Ellsworth Mountains and the occurrence of probable post-collisional anatectic granites in Tierra del Fuego imply that Patagonia was the overriding plate (Fig. 9). During deformation of the Cape Fold Belt, detrital zircon age patterns in sedimentary rocks and tuff deposits changed significantly. In the Ellsworth Mountains, volcanic tuffs in the Permian Polarstar Formation indicate nearby volcanism at *c.* 275–250 Ma (Elliot *et al.* 2016), as do similar

volcanic tuffs in the Permo-Triassic Karoo Basin, in the latter case also including some early Permian components (Fildani *et al.* 2009; Lanci *et al.* 2013; McKay *et al.* 2015).

Deformation of the Cape Fold Belt in South Africa is constrained by muscovite and biotite ^{40}Ar/^{39}Ar ages, which record two age clusters: an older one, at *c.* 275 – 260 Ma, reflects the onset of the deformation, and a younger one, at *c.* 255 – 245 Ma, may reflect either cooling of exhumed rocks or a second, younger episode of deformation (Hansma *et al.* 2016). The same ages are recorded in Tierra del Fuego, where metamorphism is dated at *c.* 265 Ma (Hervé *et al.* 2010) and post-orogenic magmatism at *c.* 255 Ma. Based on these multiple lines of evidence we propose that Permian collision between Patagonia (connected to South America and the Antarctic Peninsula) and South Africa was responsible for deformation in the Gondwanide fold belt.

Conclusions

New SHRIMP U–Pb zircon ages record the first evidence of late Permian (*c.* 255 Ma) magmatism in Tierra del Fuego, derived from melting of underlying Cambrian continental crust. This magmatism was post-orogenic with respect to the high-*T* metamorphism event reported by Hervé *et al.* (2010) in the same area.

All the studied Permian granites (with the exception of the Navarrate granite in the northern NPM) show isotopic evidence for a significant crustal component. O–Hf isotope compositions of magmatic zircons from the Tierra del Fuego samples are similar to those from contemporaneous granites in the western part of the NPM, consistent with subduction-related magmatism during the early Permian. In the northern NPM, the zircon O–Hf isotopic compositions of mid- to late Permian rocks suggest reworking of old lithosphere by more juvenile components from *c.* 280 to 255 Ma. Zircons from La Esperanza samples also record evidence for a major change in geodynamic conditions during the late Permian and early Triassic, where extensional conditions are indicated during emplacement of the felsic Calvo granite. However, contemporaneous magmatic rocks in the Yaminué Complex also indicate compressive tectonics (e.g. López de Luchi *et al.* 2010). Comparison with Late Permian magmatism from the Sierra de la Ventana suggests melting of similar crust. Together with other geological considerations, this is in line with an autochthonous or parautochthonous origin of the northern NPM.

Our data also confirm a connection between southern Patagonia and the Antarctic Peninsula from late Palaeozoic to Jurassic times: these two regions exhibit similar records of Permian magmatism and metamorphism. In Jurassic times, before the break-up of Gondwana, sources in Tierra del Fuego shed detritus to the northern Antarctic Peninsula.

Finally, this study highlights the utility (in fact the necessity) of using combined isotopic signals in zircons of igneous rocks for tracing or evaluating tectonic processes. Our data also suggest that interpretations based on Hf model ages need careful evaluation, even when δ^{18}O in zircon has a mantle-like signature.

References

Augustsson, C., Munker, C., Bahlburg, H. & Fanning, C.M. 2006. Provenance of late Palaeozoic metasediments of the SW South American Gondwana margin: a combined U–Pb and Hf-isotope study of single detrital zircons. *Journal of the Geological Society, London*, **163**, 983–995, https://doi.org/10.1144/0016-76492005-149

Batchelor, R.A. & Bowden, P. 1985. Petrogenetic interpretation of granitoid rock series using multicationic parameters. *Chemical Geology*, **48**, 43–55.

Black, L.P., Kamo, S.L., Allen, C.M., Aleinikoff, J.N., Davis, D.W., Korsch, R.J. & Foudoulis, C. 2003. TEMORA 1: a new zircon standard for Phanerozoic U–Pb geochronology. *Chemical Geology*, **200**, 155–170.

Black, L.P., Kamo, S.L. *et al.* 2004. Improved ^{206}Pb/^{238}U microprobe geochronology by the monitoring of a trace-element-related matrix effect; SHRIMP, ID-TIMS, ELA-ICP-MS and oxygen isotope documentation for a series of zircon standards. *Chemical Geology*, **205**, 115–140.

Castillo, P., Lacassie, J.P., Augustsson, C. & Hervé, F. 2015. Petrography and geochemistry of the Carboniferous–Triassic Trinity Peninsula Group, West Antarctica: Implications for provenance and tectonic setting. *Geological Magazine*, **152**, 575–588.

Castillo, P., Fanning, C.M., Hervé, F. & Lacassie, J.P. 2016. Characterisation and tracing of Permian magmatism in the south-western segment of the Gondwanan margin; U–Pb age, Lu–Hf and O isotopic compositions of detrital zircons from metasedimentary complexes of northern Antarctic Peninsula and western Patagonia. *Gondwana Research*, **36**, 1–13.

Chernicoff, C.J. & Caminos, R. 1996. Estructura y relaciones estratigráficas de la Formación Nahuel Niyeu, Macizo Norpatagónico oriental, Provincia de Río Negro. *Revista de la Asociación Geológica Argentina*, **51**, 201–212.

Chernicoff, C.J., Zappettini, E.O., Santos, J.O.S., McNaughton, N.J. & Belousova, E. 2013. Combined U–Pb SHRIMP and Hf isotope study of the Late Paleozoic Yaminué Complex, Rio Negro Province, Argentina: Implications for the origin and evolution of the Patagonia composite terrane. *Geoscience Frontiers*, **4**, 37–56.

Curtis, M.L. 2001. Tectonic history of the Ellsworth Mountains, West Antarctica: Reconciling a Gondwana enigma. *Geological Society of America Bulletin*, **113**, 939–958.

Dahlquist, J.A., Pankhurst, R.J. *et al.* 2008. New SHRIMP U–Pb data from the Famatina Complex: constraining Early–Mid Ordovician Famatinian magmatism in the Sierras Pampeanas, Argentina. *Geologica Acta*, **6**, 319–333.

Dalziel, I.W.D., Lawver, L.A. & Murphy, J.B. 2000. Plumes, orogenesis, and supercontinental fragmentation. *Earth and Planetary Science Letters*, **178**, 1–11.

Dalziel, I.W.D., Lawver, L.A., Norton, I.O. & Gahagan, L.M. 2013. The Scotia Arc: genesis, evolution, global significance. *Annual Review of Earth and Planetary Sciences*, **41**, 767–793.

Debrenne, F. 1992. The archaeocyathan fauna from the Whiteout Conglomerate, Ellsworth Mountains, West Anatarctica. *In*: Webers, G.F., Craddock, C. & Splettstoesser, J.F. (eds) *Geology and Paleontology of the Ellsworth Mountains, West Antarctica*. Geological Society of America, Memoirs, **170**, 279–284.

Deckart, K., Hervé, F., Fanning, C.M., Ramírez, V., Calderón, M. & Godoy, E. 2014. U–Pb geochronology and Hf–O isotopes of zircons from the Pennsylvanian Coastal Batholith, South–Central Chile. *Andean Geology*, **41**, 49–82.

del Rey, A., Deckart, K., Arriagada, C. & Martínez, F. 2016. Resolving the paradigm of the late Paleozoic–Triassic Chilean magmatism: Isotopic approach. *Gondwana Research*, **37**, 172–181.

Dhuime, B., Hawkesworth, C.J., Cawood, P.A. & Storey, C.D. 2012. A change in the geodynamics of continental growth 3 billion years ago. *Science*, **335**, 1334–1336.

Du Toit, A.L., 1937. *Our Wandering Continents: an Hypothesis of Continental Drifting*. Oliver & Boyd, Edinburgh.

Eggins, S.M., Grun, R. *et al.* 2005. *In situ* U-series dating by laser-ablation multi-collector ICPMS: new prospects for Quaternary geochronology. *Quaternary Science Reviews*, **24**, 2523–2538.

Elliot, D.H., Fanning, C.M. & Laudon, T.S. 2016. The Gondwana Plate margin in the Weddell Sea sector: Zircon geochronology of Upper Paleozoic (mainly Permian) strata from the Ellsworth Mountains and eastern Ellsworth Land, Antarctica. *Gondwana Research*, **29**, 234–247.

Fanning, C.M., Hervé, F., Pankhurst, R.J., Rapela, C.W., Kleiman, L.E., Yaxley, G.M. & Castillo, P. 2011. Lu–Hf isotope evidence for the provenance of Permian detritus in accretionary complexes of western Patagonia and the northern Antarctic Peninsula region. *Journal of South American Earth Sciences*, **32**, 485–496.

Fildani, A., Weislogel, A. *et al.* 2009. U–Pb zircon ages from the southwestern Karoo Basin, South Africa—Implications for the Permian–Triassic boundary. *Geology*, **37**, 719–722.

Frost, B.R., Barnes, C.G., Collins, W.J., Arculus, R.J., Ellis, D.J. & Frost, C.D. 2001. A geochemical classification for granitic rocks. *Journal of Petrology*, **42**, 2033–2048.

Ghidella, M.E., Yánez, G. & LaBrecque, J.L. 2002. Revised tectonic implications for the magnetic anomalies of the western Weddell Sea. *Tectonophysics*, **347**, 65–86.

González, P.D., Tortello, M.F. & Domborenea, S.E. 2011. Early Cambrian archaeocyathan limestone block in low-grade meta-conglometare from El Jagüelito Formation (Sierra Grande, Río Negro, Argentica). *Geologica Acta*, **9**, 159–173.

González, P.D., Tortello, M.F., Damborenea, S.E., Naipauer, M., Sato, A.M. & Varela, R. 2013. Archaeocyaths from South America: review and a new record. *Geological Journal*, **48**, 114–125.

Gregori, D.A., Grecco, L.E. & Llambías, E. 2003. El intrusivo López Lecube: Evidencias de magmatismo alcalino Gondwánico en el sector sudoeste de la provincia de Buenos Aires, Argentina. *Revista de la Asociación Geológica Argentina*, **58**, 167–175.

Gregori, D.A., Kostadinoff, J., Strazzere, L. & Raniolo, A. 2008. Tectonic significance and consequences of the Gondwanide orogeny in northern Patagonia, Argentina. *Gondwana Research*, **14**, 429–450.

Gregori, D.A., Saini-Eidukat, B., Benedini, L., Strazzere, L., Barros, M. & Kostadinoff, J. 2016. The Gondwana Orogeny in northern North Patagonian Massif: Evidences from the Caita Có granite, La Seña and Pangaré mylonites, Argentina. *Geoscience Frontiers*, **7**, 621–638.

Hansma, J., Tohver, E., Schrank, C., Jourdan, F. & Adams, D. 2016. The timing of the Cape Orogeny: New ^{40}Ar/^{39}Ar age constraints on deformation and cooling of the Cape Fold Belt, South Africa. *Gondwana Research*, **32**, 122–137.

Hawkesworth, C.J. & Kemp, A.I.S. 2006. Using hafnium and oxygen isotopes in zircons to unravel the record of crustal evolution. *Chemical Geology*, **226**, 144–162.

Henderson, R.A., Debrenne, F., Rowell, A.J. & Webers, G.F. 1992. Brachiopods, archaeocyathids, and Pelmatozoa from the Minaret Formation of the Ellsworth Mountains, West Antarctica. *In*: Webers, G.F., Craddock, C. & Splettstoesser, J.F. (eds) *Geology and Paleontology of the Ellsworth Mountains, West Antarctica*. Geological Society of America, Memoirs, **170**, 249–268.

Hervé, F., Fanning, C.M. & Pankhurst, R.J. 2003. Detrital zircon age patterns and provenance of the metamorphic complexes of southern Chile. *Journal of South American Earth Sciences*, **16**, 107–123.

Hervé, F., Miller, H. & Pimpirev, C. 2005. Patagonia–Antarctica connections before Gondwana break-up. *In*: Fütterer, D., Damaske, D., Kleinschmidt, G., Miller, H. & Tessensohn, F. (eds) *Antarctica: Contribution to Global Earth Sciences*. Springer, Berlin, 217–228.

Hervé, F., Calderón, M., Fanning, C.M., Kraus, S. & Pankhurst, R.J. 2010. SHRIMP chronology of the Magallanes Basin basement, Tierra del Fuego: Cambrian plutonism and Permian high-grade metamorphism. *Andean Geology*, **37**, 253–275.

Hervé, F., Calderón, M., Fanning, C.M., Pankhurst, R.J. & Godoy, E. 2013. Provenance variations in the Late Paleozoic accretionary complex of central Chile as indicated by detrital zircons. *Gondwana Research*, **23**, 1122–1135.

Hervé, F., Fanning, C.M., Calderón, M. & Mpodozis, C. 2014. Early Permian to Late Triassic batholiths of the Chilean Frontal Cordillera (28°–31°S): SHRIMP U–Pb zircon ages and Lu–Hf and O isotope systematics. *Lithos*, **184–187**, 436–446.

Iannizzotto, N.F., Rapela, C.W., Baldo, E.G.A., Galindo, C., Fanning, C.M. & Pankhurst, R.J. 2013. The Sierra Norte-Ambargasta batholith: Late Ediacaran–Early Cambrian magmatism associated with Pampean transpressional tectonics. *Journal of South American Earth Sciences*, **42**, 127–143.

Ickert, R.B., Hiess, J. *et al*. 2008. Determining high precision, *in situ*, oxygen isotope ratios with a SHRIMP II: Analyses of MPI-DING silicate-glass reference materials and zircon from contrasting granites. *Chemical Geology*, **257**, 114–128.

Kay, S.M., Ramos, V.A., Mpodozis, C. & Sruoga, P. 1989. Late Paleozoic to Jurassic silicic magmatism at the Gondwana margin: analogy to the Middle Proterozoic in North America? *Geology*, **17**, 324–328.

Kemp, A.I.S., Hawkesworth, C.J., Paterson, B.A. & Kinny, P.D. 2006. Episodic growth of the Gondwana supercontinent from hafnium and oxygen isotopes in zircon. *Nature*, **439**, 580–583.

Kemp, A.I.S., Hawkesworth, C.J. *et al*. 2007. Magmatic and crustal differentiation history of granitic rocks from Hf–O isotopes in zircon. *Science*, **315**, 980–983.

Kemp, A.I.S., Hawkesworth, C.J., Collins, W.J., Gray, C.M. & Blevin, P.L. 2009. Isotopic evidence for rapid continental growth in an extensional accretionary orogen: The Tasmanides, eastern Australia. *Earth and Planetary Science Letters*, **284**, 455–466.

Kleiman, L.E. & Japas, M.S. 2009. The Choiyoi volcanic province at 34°S–36°S (San Rafael, Mendoza, Argentina): Implications for the Late Palaeozoic evolution of the southwestern margin of Gondwana. *Tectonophysics*, **473**, 283–299.

König, M. & Jokat, W. 2006. The Mesozoic breakup of the Weddell Sea. *Journal of Geophysical Research: Solid Earth*, **111**, 1–28.

Labudía, C.H. & Bjerg, E.A. 1995. Geología del sector oriental de la hoja bajo Hondo (39e), Provincia de Río Negro. *Revista de la Asociación Geológica Argentina*, **49**, 284–296.

Lanci, L., Tohver, E., Wilson, A. & Flint, S. 2013. Upper Permian magnetic stratigraphy of the lower Beaufort Group, Karoo Basin. *Earth and Planetary Science Letters*, **375**, 123–134.

Lawver, L.A., Gahagan, L.M. & Dalziel, W.D. 1998. A tight fit—early Mesozoic Gondwana, a plate reconstruction perspective. *Memoirs of the National Institute for Polar Research*, **53**, 214–228.

Llambías, E.J. & Rapela, C.W. 1984. Geología de los complejos eruptivos de la Esperanza, provincia de Río Negro. *Revista de la Asociación Geológica Argentina*, **39**, 220–243.

Llambías, E.J., Leanza, H.A. & Carbone, O. 2007. Evolución tectono-magmática durante el Pérmico al Jurásico temprano en la Cordillera del Viento (37°05′S–37°15′S): nuevas evidencias geológicas y geoquímicas del inicio de la cuenca Neuquina. *Revista de la Asociación Geológica Argentina*, **62**, 217–235.

López de Luchi, M.G. & Cerredo, M.E. 2008. Geochemistry of the Mamil Choique granitoids at Río Chico, Río Negro, Argentina: Late Paleozoic crustal melting in the North Patagonian Massif. *Journal of South American Earth Sciences*, **25**, 526–546.

López de Luchi, M.G., Rapalini, A.E. & Tomezzoli, R.N. 2010. Magnetic fabric and microstructures of Late Paleozoic granitoids from the North Patagonian Massif: Evidence of a collision between Patagonia and Gondwana? *Tectonophysics*, **494**, 118–137.

López-Gamundí, O., Fildani, A., Weislogel, A. & Rossello, E.A. 2013. The age of the Tunas formation in the Sauce Grande basin–Ventana foldbelt (Argentina): Implications for the Permian evolution of the southwestern margin of Gondwana. *Journal of South American Earth Sciences*, **45**, 250–258.

Maksaev, V., Munizaga, F. & Tassinari, C. 2014. Timing of the magmatism of the paleo-Pacific border of Gondwana: U–Pb geochronology of Late Paleozoic to Early Mesozoic igneous rocks of the north Chilean Andes between 20° and 31°S. *Andean Geology*, **41**, 447–506.

Maniar, P.D. & Piccoli, P.M. 1989. Tectonic discrimination of granitoids. *Geological Society of America Bulletin*, **101**, 635–643.

Martínez Dopico, C.I., López de Luchi, M., Wemmer, K. & Rapalini, A.E. 2013. Composición química de biotita y hornblenda y edades de enfriamiento como indicadores de las condiciones de emplazamiento del Complejo Plutónico La Esperanza (Pérmico Superior), Macizo Norpatagónico. *Revista de la Asociación Geológica Argentina*, **70**, 3–15.

McKay, M.P., Weislogel, A.L., Fildani, A., Brunt, R.L., Hodgson, D.M. & Flint, S.S. 2015. U–Pb zircon tuff geochronology from the Karoo Basin, South Africa: implications of zircon recycling on stratigraphic age controls. *International Geology Review*, **57**, 393–410.

Millar, I.L., Pankhurst, R.J. & Fanning, C.M. 2002. Basement chronology of the Antarctic Peninsula: recurrent magmatism and anatexis in the Palaeozoic Gondwana Margin. *Journal of the Geological Society, London*, **159**, 145–157, https://doi.org/10.1144/0016-764901-020

Mundl, A., Ntaflos, T., Ackerman, L., Bizimis, M., Bjerg, E.A. & Hauzenberger, C.A. 2015. Mesoproterozoic and Paleoproterozoic subcontinental lithospheric mantle domains beneath southern Patagonia: Isotopic evidence for its connection to Africa and Antarctica. *Geology*, **43**, 39–42.

Munizaga, F., Maksaev, V., Fanning, C.M., Giglio, S., Yaxley, G. & Tassinari, C. C.G. 2008. Late Paleozoic–Early Triassic magmatism on the western margin of Gondwana: Collahuasi area, Northern Chile. *Gondwana Research*, **13**, 407–427.

Nebel, O., Vroon, P.Z., van Westrenen, W., Iizuka, T. & Davies, G.R. 2011. The effect of sediment recycling in subduction zones on the Hf isotope character of new arc crust, Banda arc, Indonesia. *Earth and Planetary Science Letters*, **303**, 240–250.

Paces, J.B. & Miller, J.D. 1993. Precise U–Pb ages of Duluth complex and related mafic intrusions, northeastern Minnesota: Geochronological insights to physical, petrogenetic, paleomagnetic, and tectonomagmatic processes associated with the 1.1 Ga midcontinental rift system. *Journal of Geophysical Research*, **98**, 13997–14013.

Pankhurst, R.J., Rapela, C.W., Caminos, R., Llambías, E.J. & Párica, C. 1992. A revised age for the granites of the central Somuncura batholith, North Patagonian Massif. *Journal of South American Earth Sciences*, **5**, 321–325.

Pankhurst, R.J., Rapela, C.W., Saavedra, J., Baldo, E., Dahlquist, J., Pascua, I. & Fanning, C.M. 1998. The Famatinian magmatic arc in the southern Sierras Pampeanas. *In*: Pankhurst, R.J. & Rapela, C.W. (eds) *The Proto-Andean Margin of Gondwana*. Geological Society, London, Special Publications, **142**, 343–367, https://doi.org/10.1144/GSL.SP.1998.142.01.17

Pankhurst, R.J., Rapela, C.W., Loske, W.P., Márquez, M. & Fanning, C.M. 2003. Chronological study of the pre-Permian basement rocks of southern Patagonia. *Journal of South American Earth Sciences*, **16**, 27–44.

Pankhurst, R.J., Rapela, C.W., Fanning, C.M. & Márquez, M. 2006. Gondwanide continental collision and the origin of Patagonia. *Earth-Science Reviews*, **76**, 235–257.

Pankhurst, R.J., Rapela, C.W., López De Luchi, M.G., Rapalini, A.E., Fanning, C.M. & Galindo, C. 2014. The Gondwana connections of northern Patagonia. *Journal of the Geological Society, London*, **171**, 313–328, https://doi.org/10.1144/jgs2013-081

Payne, J.L., McInerney, D.J., Barovich, K.M., Kirkland, C.L., Pearson, N.J. & Hand, M. 2016. Strengths and limitations of zircon Lu–Hf and O isotopes in modelling crustal growth. *Lithos*, **248–251**, 175–192.

Ramos, V.A. 1984. Patagonia, Un continente paleozoico a la deriva? *Actas del noveno Congreso Geológico Argentino, Tomo II*, Asociación geológica Argentina, San Carlos de Bariloche, 311–325.

Ramos, V.A. 2008. Patagonia: A Paleozoic continent adrift? *Journal of South American Earth Sciences*, **26**, 235–251.

Ramos, V.A. & Naipauer, M. 2014. Patagonia: where does it come from? *Journal of Iberian Geology*, **40**, 367–379.

Ramos, V.A., Chemale, F., Naipauer, M. & Pazos, P.J. 2014. A provenance study of the Paleozoic Ventania System (Argentina): Transient complex sources from Western and Eastern Gondwana. *Gondwana Research*, **26**, 719–740.

Rapalini, A.E. 2005. The accretionary history of southern South America from the latest Proterozoic to the late Paleozoic: some paleomagnetic constraints. *In*: Vaughan, A.P.M., Leat, P.T. & Pankhurst, R.J. (eds) *Terrane Processes at the Margins of Gondwana*. Geological Society, London, Special Publications, **246**, 305–328, https://doi.org/10.1144/GSL.SP.2005.246.01.12

Rapalini, A.E., López de Luchi, M.G., Tohver, E. & Cawood, P.A. 2013. The South American ancestry of the North Patagonian Massif: geochronological evidence for an autochthonous origin? *Terra Nova*, **25**, 337–342.

Rapela, C.W. & Caminos, R. 1987. Geochemical characteristics of the Upper Paleozoic magmatism in the eastern sector of North Patagonian Massif. *Revista Brasileira de Geociencias*, **17**, 535–542.

Rapela, C.W. & Llambias, E. 1985. Evolucion magmatica y relaciones regionales de los complejos eruptivo de La Esperanza, Provincia de Rio Negro. *Revista de la Asociación Geológica Argentina*, **40**, 4–25.

Rapela, C.W., Pankhurst, R.J., Casquet, C., Baldo, E., Saavedra, J., Galindo, C. & Fanning, C.M. 1998. The Pampean orogeny of the southern proto-Andes: Cambrian continental collision in the Sierras de Córdoba. *In*: Pankhurst, R.J. & Rapela, C.W. (eds) *The Proto-Andean Margin of Gondwana*. Geological Society, London, Special Publications, **142**, 181–217, https://doi.org/10.1144/GSL.SP.1998.142.01.10

Rapela, C.W., Pankhurst, R.J., Fanning, C.M. & Grecco, L.E. 2003. Basement evolution of the Sierra de la Ventana Fold Belt: new evidence for Cambrian continental rifting along the southern margin of Gondwana. *Journal of the Geological Society, London*, **160**, 613–628, https://doi.org/10.1144/0016-764902-112

Riley, T.R., Flowerdew, M.J. & Whitehouse, M.J. 2012. U–Pb ion-microprobe zircon geochronology from the basement inliers of eastern Graham Land, Antarctic Peninsula. *Journal of the Geological Society, London*, **169**, 381–393, https://doi.org/10.1144/0016-76492011-142

Rocha-Campos, A.C., Basei, M.A. *et al.* 2011. 30 million years of Permian volcanism recorded in the Choiyoi igneous province (W Argentina) and their source for younger ash fall deposits in the Paraná Basin: SHRIMP U–Pb zircon geochronology evidence. *Gondwana Research*, **19**, 509–523.

Schilling, M.E., Carlson, R.W., Conceição, R.V., Dantas, C., Bertotto, G.W. & Koester, E. 2008. Re–Os isotope constraints on subcontinental lithospheric mantle evolution of southern South America. *Earth and Planetary Science Letters*, **268**, 89–101.

Sölner, F., Miller, H. & Hervé, F. 2000. An Early Cambrian granodiorite age from the pre-Andean basement of Tierra del Fuego (Chile): the missing link between South America and Antarctica? *Journal of South American Earth Sciences*, **13**, 163–177.

Stone, P. & Thomson, M.R.A. 2005. Archaeocyathan limestone blocks of likely Antarctic origin in Gondwanan tillite from the Flakland Islands. *In*: Vaughan, A.P.M., Leat, P.T. & Pankhurst, R.J. (eds) *Terrane Processes at the Margins of Gondwana*. Geological Society, London, Special Publications, **246**, 347–357, https://doi.org/10.1144/GSL.SP.2005.246.01.14

Stone, P., Thomson, M.R.A. & Rushton, A.W.A. 2012. An Early Cambrian archaeocyath–trilobite fauna in limestone erratics from the Upper Carboniferous Fitzroy Tillite Formation, Falkland Islands. *Earth and Environmental Science Transactions of the Royal Society of Edinburgh*, **102**, 201–225.

Tohver, E., Cawood, P.A., Rossello, E.A., López de Luchi, M.G., Rapalini, A.E. & Jourdan, F. 2008. New SHRIMP U–Pb and ^{40}Ar/^{39}Ar constraints on the crustal stabilization of southern South America, from the margin of the Rio de Plata (Sierra de Ventana) craton to northern Patagonia. *EOS Transactions, American Geophysical Union, Fall Meetings*, T23C-2052.

Valley, J.W., Lackey, J.S. *et al.* 2005. 4.4 billion years of crustal maturation: oxygen isotope ratios of magmatic zircon. *Contributions to Mineralogy and Petrology*, **150**, 561–580.

Vervoort, J.D. & Blichert-Toft, J. 1999. Evolution of the depleted mantle: Hf isotope evidence from juvenile rocks through time. *Geochimica et Cosmochimica Acta*, **63**, 533–556.

Vervoort, J.D. & Kemp, A.I.S. 2016. Clarifying the zircon Hf isotope record of crust–mantle evolution. *Chemical Geology*, **425**, 65–75.

Vervoort, J.D., Patchett, P.J., Blichert-Toft, J. & Albarède, F. 1999. Relationships between Lu–Hf and Sm–Nd isotopic systems in the global sedimentary system. *Earth and Planetary Science Letters*, **168**, 79–99.

von Gosen, W. 2003. Thrust tectonics in the North Patagonian Massif (Argentina): Implications for a Patagonia plate. *Tectonics*, **22**, 1005.

Williams, I.S. 1998. U–Th–Pb geochronology by ion microprobe. *In*: McKibben, M.A., Shanks, W.C., III & Ridley, W.I. (eds) *Application of Microanalytical Techniques to Understanding Mineralizing Processes*. Society of Economic Geologists, Reviews of Economic Geology, **7**, 1–35.

Willner, A.P., Glodny, J., Gerya, T.V., Godoy, E. & Massonne, H.J. 2004. A counterclockwise *PTt* path of high-pressure/low-temperature rocks from the Coastal Cordillera accretionary complex of south–central Chile: constraints for the earliest stage of subduction mass flow. *Lithos*, **75**, 283–310.

Yrigoyen, M. 1999. Los depósitos cretácicos y terciarios de las cuencas del Salado y del Colorado. *In*: Caminos, R. (ed.) *Geología Argentina*. Servicio Geológico Minero. Instituto de Geología y Recursos Naturales, **29**. Buenos Aires, 645–650.